Probing Cage Relaxation in Concentrated Protein Solutions by X-Ray Photon Correlation Spectroscopy

Yuriy Chushkin,[1,*] Alessandro Gulotta,[2] Felix Roosen-Runge,[2,3] Antara Pal,[2] Anna Stradner,[2,4] and Peter Schurtenberger[2,4,†]

[1]*ESRF, The European Synchrotron, 71 Avenue des Martyrs, CS40220, 38043 Grenoble Cedex 9, France*
[2]*Division of Physical Chemistry, Lund University, Naturvetarvägen 14, 22100 Lund, Sweden*
[3]*Department of Biomedical Science and Biofilms Research Center for Biointerfaces (BRCB), Faculty of Health and Society, Malmö University, Sweden*
[4]*Lund Institute of advanced Neutron and X-ray Science LINXS, Lund University, Lund, Sweden*

(Received 28 March 2022; accepted 21 October 2022; published 29 November 2022)

Diffusion of proteins on length scales of their size is crucial for understanding the machinery of living cells. X-ray photon correlation spectroscopy (XPCS) is currently the only way to access long-time collective diffusion on these length scales, but radiation damage so far limits the use in biological systems. We apply a new approach to use XPCS to measure cage relaxation in crowded α-crystallin solutions. This allows us to correct for radiation effects, obtain missing information on long time diffusion, and support the fundamental analogy between protein and colloid dynamical arrest.

DOI: 10.1103/PhysRevLett.129.238001

Molecular processes leading to dynamical arrest in biomacromolecular solutions are vital for life, governing protein assembly and condensation as essential formation pathways of biological structure [1]. As examples, both the attractive gel [2] and repulsive glass transition [3] observed in concentrated protein solutions present relevant cases for optimization of pharmaceutical formulations.

Colloid science provides a successful frame to approach the questions of phase behavior and dynamics of globular protein solutions [4]. In colloid and glass physics, the mechanistic understanding of dynamical arrest during glass formation or gelation has been established by complementing information on multiscale structure with results on macroscopic viscosity and local diffusion, including particularly caging processes [5].

Since nonspherical protein conformations with anisotropic molecular interactions render naive colloidal interpretations problematic [4], a comprehensive experimental characterization of protein solutions is essential for a quantitative, mechanistic understanding. While multiscale structure and macroscopic dynamics are accessible using imaging and scattering techniques [6], diffusion on the length scale of nearest neighbors is only available on short timescales up to a few hundred nanoseconds by neutron spin-echo spectroscopy, corresponding to typical rattling-in-the-cage motions [2,7,8].

Information on longer micro- to millisecond timescales addressing out-of-cage diffusion is so far missing. Given the length scale of roughly 10 nanometers for proteins, the only experimental technique to probe the collective diffusion is x-ray photon correlation spectroscopy (XPCS) [9,10]. However, so far, applications to biological matter have been hampered by the x-ray radiation damage [10,11]. The conventional approach has been to limit the deposited dose below a critical value [10,12], before structural changes become measurable. Low dose XPCS requires distribution of the radiation over a large sample volume to optimize the scattered signal [11]. For example, using a 100×100 μm large beam, collective dynamics at long length scales could be addressed in concentrated antibody formulations [13]. Alternatively, one can translate a sample to control the dose [10,12]. By this approach, proof-of-principle results on the cage relaxation in concentrated solutions of the protein α-crystallin were reported [10], but relaxation times were limited by the translation times, and thus do not extend to the long time scales relevant close to dynamic arrest. Moreover, recent work [12] reported a five times lower critical dose for the same protein than in the earlier study [10]. It is clear that we lack sufficient understanding of the role of radiation effects in XPCS experiments with concentrated protein solutions. In this Letter we therefore address the problem of radiation-induced damage for such experiments. We show that collective long-time cage relaxation in concentrated protein solutions measured with XPCS is affected by the dose rate even below critical dose values. We characterize the beam-induced dynamics

and demonstrate a specific experimental design and analysis strategy that correctly estimates the intrinsic solution dynamics in agreement with existing rheology data. Furthermore, we discuss the role of the underlying processes responsible for the observed radiation effects.

The SAXS and XPCS measurements were performed at the ID10 beam line. We benefit from a ~100 fold increase in the coherent fraction of the recently upgraded extremely brilliant source (EBS) at the ESRF [14]. We used 9.5 keV radiation selected by a Si(111) channel-cut monochromator and beam sizes of 20×20 or 30×30 μm^2 with high spatial coherence. The maximum intensity was 3.74×10^{11} and 2.45×10^{10} ph/s for the focused and unfocused beam. Si attenuators were inserted to reduce the absorbed dose and the dose rate. The deposited dose was calculated following [15]. Scattering patterns were recorded by the Eiger 500*K* detector [16] placed 6.9 m downstream from a sample and shifted to access the static structure peak. This setup with a high coherent fraction provides ideal conditions to systematically explore effects of dose rate and dose, and test whether physical information on collective solution dynamics can be reliably extracted.

We used concentrated solutions of the protein α-crystallin [17] from the bovine eye lens as a model system. Importantly, α-crystallin has been extensively studied using light scattering, small-angle x-ray scattering, neutron spin echo and macro- and microrheology [2,3,18], all of which support a coherent picture for the solution structure, collective diffusion, and the glass transition based on a model of polydisperse hard spheres. XPCS measurements on this system presents the ideal experiment to complete the physical characterization with the missing information on long-time cage relaxation, and at the same time test the potential of XPCS for crowded protein solutions.

We prepared a series of concentrations following a protocol [2] in a concentration range between 300 and 360 mg/ml, corresponding to a protein volume fraction ϕ between 0.51 and 0.61 [3]. As a solvent we use a 52.4 mM phosphate buffer (pH 7.1) with 20 mM DTT (dithiothreitol) and 1 mM EDTA (ethylenediaminetetraacetic acid) to reduce effects of oxidative stress and radiation damage, for more details see the Supplemental Material [19]. The samples were sealed in quartz capillaries with 1.5 mm diameter, and measured at room temperature. We used ~10 to ~1000 fresh spots per sample with 60 μm spacing, and collected series of 500 to 20 000 frames for each spot to achieve good signal-to-noise ratios. For each sample several datasets with different beam intensity and acquisition time were acquired.

All samples show a correlation peak in the small-angle scattering curve [Fig. S1(a) [19]]. Fitting this by the product of the low concentration form factor of α-crystallin and a structure factor for a polydisperse hard-sphere model [20], we extract the peak height $S(q^*)$ and the peak position q^* to monitor beam-induced structural changes.

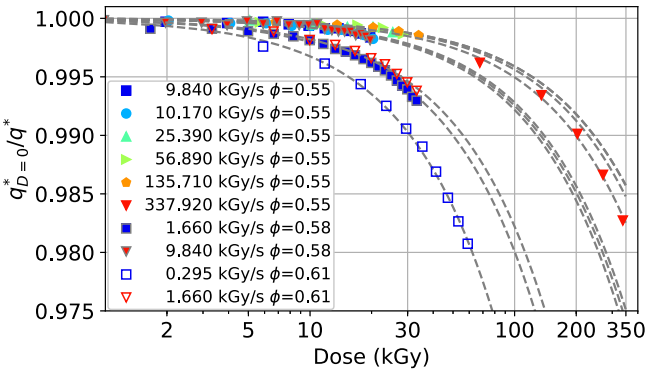

FIG. 1. Inverse of the relative position $q^*_{D=0}/q^*$ of the peak in the structure factor $S(q)$, where $q^*_{D=0}$ is the extrapolated zero-dose limit, as a function of deposited dose and dose rate for α-cystallin solutions at different volume fractions ϕ. The guides to the eye (gray dashed) are exponential decays.

Fig. 1 shows the inverse of the extracted parameter q^* normalized to the zero-dose limit $q^*_{D=0}$ versus the deposited dose. In the calculation of $q^*_{D=0}$ we assumed an exponential decay (dashed lines). With increasing dose, $S(q^*)$ decreases [Fig. S1(c) [19]] and q^* shifts to larger values. Importantly, the rate of change is not constant but depends on the dose rate and volume fraction [Fig. S1(d) [19]], explaining the earlier conflicting findings on critical doses for α-crystallin [10,12].

Indeed, the measured intensity correlation functions $g^{(2)}(q^*,t) = \langle I(q^*,0)I(q^*,t)\rangle/\langle I(t)\rangle^2$ shown in Fig. 2 for different volume fractions are sensitive to the dose rates. A significant effect of dose rate on the decay time and shape is observed, even if the absolute dose is below 10 kGy (Fig. 2). To quantify this observation, we fitted the curves with the Kohlrausch-Williams-Watts (KWW) expression [21] $g^{(2)}(q,\tau) = 1 + c\ \exp[-2\ (\tau/\tau_r)^{\beta}]$, with the contrast factor c, and the relaxation time τ_r. The relaxation exponent β reflects the signature of the dynamical process, ranging from a stretched decay with $\beta < 1$, over a simple exponential decay with $\beta = 1$ to a compressed function with $\beta > 1$.

The dose-dependent behavior is analyzed using time-resolved $g^{(2)}$ extracted from the two-time correlation function [22] shown in Fig. S3 [19]. Both β and the average relaxation time $\langle\tau_r\rangle = (\tau_r/\beta)\Gamma(1/\beta)$ are affected by the dose and dose rate (Fig. 2). While we observe slow dynamics at low doses below the radiation damage threshold, large dose rates lead to faster dynamics, and a transition from stretched to compressed signatures. The dynamical signatures depend even stronger on dose rate than the structural features in Fig. 1: the temporal decorrelation of the structural features due to the shift of q^* (Fig. S2 [19]) is significantly slower than the beam-induced dynamics $g^{(2)}(q,\tau)$ observed in XPCS.

Interestingly, the sensitivity of the samples to radiation-induced effects seems related to the physical state. The

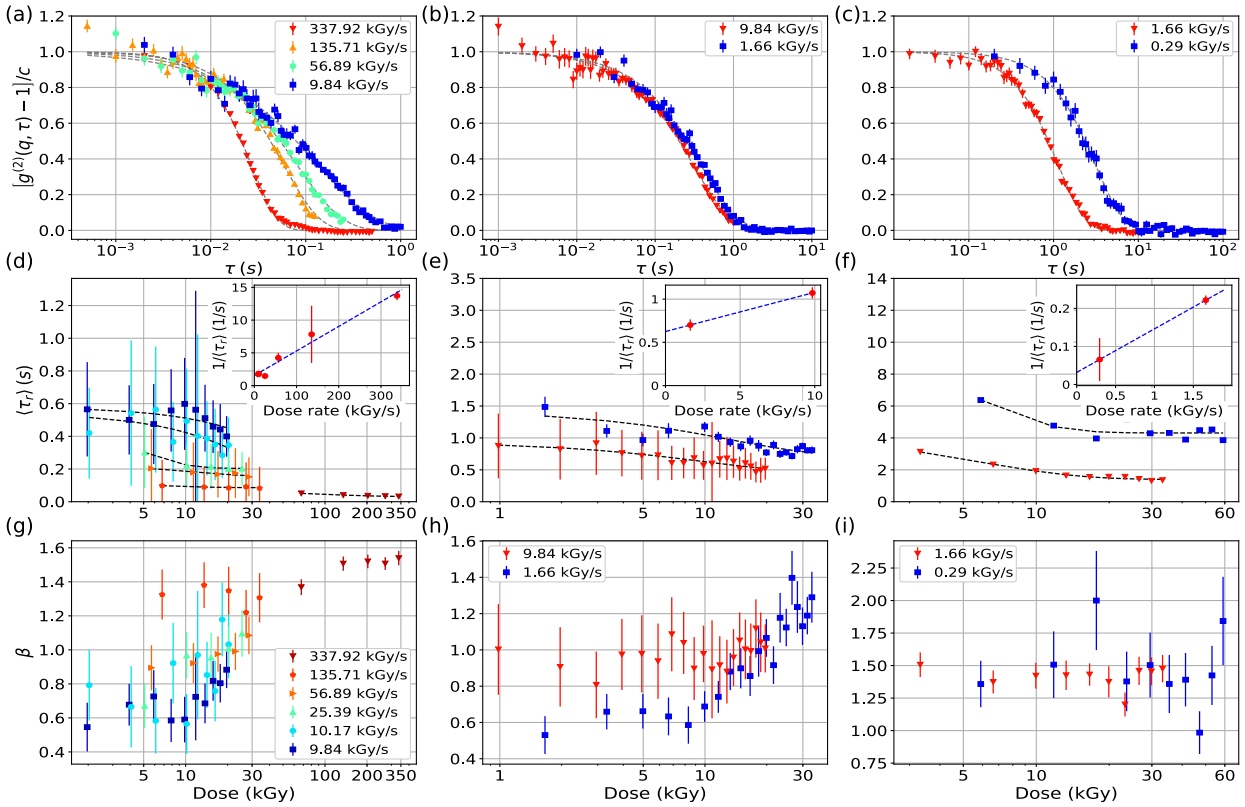

FIG. 2. Observed dynamical characteristics of α-crystallin solutions dependent on the dose and dose rates at volume fractions: $\phi = 0.55$ (left), $\phi = 0.58$ (center), $\phi = 0.61$ (right). Top: measured normalized intensity correlation functions. Dashed lines are fits with the KWW expression. Middle: the average relaxation time $\langle \tau_r \rangle$ is decreased by both dose rate and dose. Inset: the relaxation rate as a function of the dose rate. Bottom: the exponent parameter β evidences a transition from stretched exponential decay in the weakly affected fluid state to compressed decay for the strongly affected state.

sample at volume fraction $\phi = 0.55$ is close to the glass transition but still fluid, implying a stretched relaxation with $\beta < 1$ [23,24]. Indeed, both $\langle \tau_r \rangle$ and β show consistent values below 10 kGy for the smallest two dose rates around 10 kGy/s. Larger dose rates induce faster relaxations of different nature with $\beta > 1$ [Figs. 2(d) and 2(g)].

The sample at the intermediate volume fraction of 0.58 is at the arrest transition, which should result in a stretched exponential decay. While the measurement at the lowest dose rate returns a reasonable $\beta < 1$, a dose rate around 10 kGy/s already induces an inconsistent $\beta \approx 1$, implying a higher sensitivity to dose rate than for the slightly less concentrated sample.

The highest volume fraction of 0.61 corresponds to an arrested sample, which would in principle imply a constant plateau for the long-time α relaxation observed by XPCS. However, for our sample structural relaxation is induced already for much smaller dose rates around 1 kGy/s, with $\beta \approx 1.5$ and a $\langle \tau_r \rangle$ of similar magnitude as at the arrest transition. In addition, $\langle \tau_r \rangle$ does not show a constant value below 10 kGy, suggesting that the dynamical signatures are related to radiation-induced relaxation processes. For colloidal hard or soft sphere glasses one finds a final very slow decay in the correlation functions due to aging processes that result in a compressed exponential decay with $\beta \approx 1.5$, due to the relaxation of internal stresses through nondiffusive processes [25].

The beam-induced dynamics and the intrinsic dynamics are assumed to be two independent and parallel relaxation processes [26,27], motivating a correction for the effect of dose rate to extract the correct intrinsic long-time collective dynamics. By fitting with an exponential decay we determine the average relaxation rate $1/\langle \tau_r \rangle$ (at zero dose) versus dose rate (insets in Fig. 2) as proposed in [28]. The observed linear relationship of the zero-dose-limit of $1/\langle \tau_r \rangle$ versus dose rate (insets in Fig. 2) allows extrapolation to the limit of zero dose rate for our samples, which approaches the intrinsic dynamics of the system [28]. We verify this approach by comparing the estimated values with complementary measurements. The long-time α relaxation scales with the macroscopic solution viscosity. Figure 3 displays viscosities from rheology [3] and microrheology [18] along with the relaxation times normalized by the dilute limit $\tau_0 = 1/D_0 q^2$ with the diffusion coefficient $D_0 = 2.2 \times 10^{-11}$ m^2/s. The excellent agreement validates the applicability of XPCS for obtaining physical information of the undisturbed sample, if systematic corrections for dose-rate effects are performed.

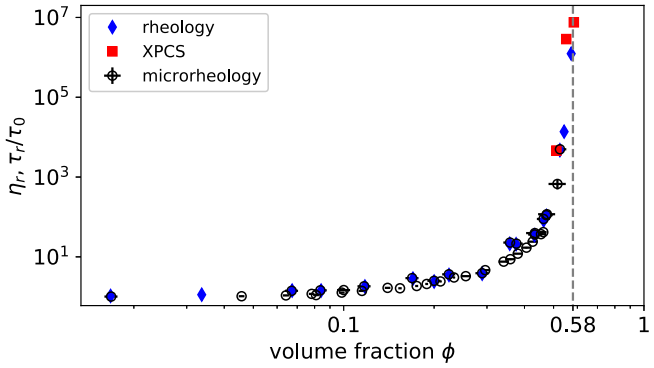

FIG. 3. Relative zero-shear viscosity η_r of α-crystallin solutions as a function of volume fraction ϕ obtained from rheology (data from [3]) and microrheology (data from [18]) and normalized relaxation times obtained from XPCS (red squares).

What remains to be discussed is the physical origin of the observed intriguing dynamics: while a stretched-exponential signature is observed in high concentration still fluid protein solutions at low dose rates, the increase of both dose rate and the protein concentration results in compressed-exponential signatures. We remark that a transition from stretched to compressed decays with a decrease of the temperature or an increase in concentration was reported in metallic [29] and colloidal [30] glasses, as well as predicted theoretically for such systems [31]. However, the dose rate does not change the relaxation signature in these systems, which seems to be a new observation in these proteins solutions, likely relevant for other radiation-sensitive biological systems.

As a likely explanation, we consider the formation of covalent links between proteins caused by radiation-induced radicals [32,33]. Upon illumination with x rays, highly reactive hydroxyl (HO) radicals are formed by the decomposition of water [34]. In concentrated protein solutions, HO almost instantaneously diffuses to and reacts with the protein surface into C-centered protein radicals. In close contact, these protein radicals react, and form permanent covalent bonds between protein molecules [33,35]. Typically, protein cluster formation results in a slowing down of diffusion, and a stretched exponential decay of the correlation function. However, we stress that our experiments do not study the equilibrium dynamics of protein clusters, but the nonequilibrium situation of protein solutions during cluster formation. The nonequilibrium nature of the radical reaction induces changes in the free energy landscape during bond creation. In particular, the close binding of two proteins leads to the opening of a local void in the nearest neighbor cages of the crowded protein solutions, into which the surrounding proteins relax with a locally directed motion (see Fig. S5 [19]). Thus, the driven process of radical bond formation is expected to induce an apparent quasiballistic motion explaining the compressed signature in the collective relaxation.

The relevance of these processes on the experimental timescales is supported by a quantitative estimation: The formation rate of radicals per protein molecule can be expressed as

$$k_r = Gj\frac{\rho_{H_2O}V_{\text{beam}}}{N_p} \approx \frac{0.68}{s}\frac{j}{kGy/s}, \tag{1}$$

where j is the equivalent dose rate, $G = 2.8 \times 10^{-7}$ mol J^{-1} expresses the number of hydroxyl radicals per absorbed radiation dose [34], $\rho_{H_2O} \approx 1$ g/ml is the water density, and $V_{\text{beam}} = 30\,\mu\text{m} \times 30\,\mu\text{m} \times 1.5\,\text{mm}$ is the illuminated beam volume. The number of proteins $N_p = V_{\text{beam}}c_p/M_w \approx 5.6 \times 10^{-13}$ mol has been evaluated for realistic values for the protein mass concentration $c_p \approx 330$ mg/ml, and a molecular weight of $M_w \approx 800$ kDa. For a dose rate of 10 kGy/s, the proteins obtain on average one radical every $\tau_r = 1/k_r \approx 150$ ms.

The confinement of a protein in a dense cage of other proteins implies that rotational tumbling and translational collision times are on microsecond timescales, while out-of-cage diffusion is orders of magnitudes slower. The first radical bonds form with a rate $k_b \approx 10^5/\text{s} \gg k_r$ as soon as two neighboring proteins receive one radical each. An estimation for the average time for one bond formation per protein reads $\tau_b = 2/k_r \approx 300$ ms, which is consolidated by rate equations [19].

The formation of subsequent bonds slows down considerably, as cluster formation obstructs the rotation and translation of proteins needed to find neighboring radicals. Our simple consideration rationalized why nonequilibrium driven motions induced by x-ray radiation should be expected in these dense proteins on time scales of 100 ms to seconds.

For liquid samples close to dynamical arrest, this proposed mechanism explains why the long-time relaxation of $g^{(2)}(q,\tau)$ changes from a stretched to a compressed exponential behavior, while for the already arrested nonergodic samples all correlation functions measured are compressed with a characteristic relaxation time accelerating with increased absorbed radiation. It is also consistent with our observations that the position q^* of the nearest neighbor peak increases and the corresponding peak amplitude $S(q^*)$ decreases with increasing dose, as these quantities reflect the increasing number of defects created in the cage structure caused by radical bond formation between proteins and the concomitant decrease of the average nearest neighbor distance.

We stress that this picture might be different for lower volume fractions, where radiation-induced clustering has been speculated about based on radiation-induced slowing down [36,37]. Under these conditions we expect that radiation-induced aggregation would exhibit the typical features of reaction-limited cluster-cluster aggregation [38] and strongly interfere with our ability to measure collective

dynamics on longer timescales with XPCS. In contrast, at very high concentrations close to dynamical arrest, the proposed mechanism is instead related to percolation [39]. Here the large difference between short-time diffusion rattling in the nearest neighbor cage, and long-time diffusion caused by cage relaxation only allows for bond formation between nearest-neighbor proteins, and cluster diffusion over longer distances is prohibited by the cages.

We note that the beam-induced dynamics is of non-thermal nature, as from finite difference calculations [40] for the highest dose rate we obtain a maximum heating of ~0.44 °C [Fig. S4(b) [19]].

In conclusion, using the highly coherent x-ray beam of the EBS source we collected high-quality XPCS data on concentrated α-crystallin solutions. By applying a systematic approach—varying dose and dose rate—we reveal information on the physical mechanism behind dynamical arrest on nearest-neighbor length scale that with previous studies completes the colloidal picture of dynamical arrest of α-crystallin. We obtained indirect information on the mechanism behind structural changes and dynamical acceleration induced by x-ray radiation. We showed that the dose rate is the relevant parameter to control in the XPCS measurements in addition to the dose. In essence, access to the true microscopic dynamics of biological samples is possible, if experiments stay both below the critical dose and the dose rate. Importantly, the critical dose rate seems to be related to the ratio of the critical dose to the relaxation time of the system. Therefore, an experimental characterization of short-time cage diffusion may even be possible with XPCS when using sufficiently intense x-ray beams where the absorbed dose would be above the typical estimate of the critical dose of 10 kGy, but where bond formation would be sufficiently delayed due to the significant difference between short-time diffusion and bond formation. Given the enormous improvements of coherent beam characteristics at modern synchrotron sources, XPCS in this spirit is highly promising for future in-depth characterization of local dynamics in biological and soft materials.

This research was financially supported by the Swedish National Research Council (Vetenskapsrådet) under Grant No. 2016-03301, the Röntgen-Ångström Cluster Grant No. 2019-06075, and the Crafoord Foundation (Lund, Sweden). We acknowledge support by LINXS—Lund Institute of Advanced Neutron and X-ray Science. Md. Arif Kamal, T. Narayanan, and T. Zinn are acknowledged for fruitful discussions and help. The authors would like to thank F. Zontone for technical assistance during the experiment. We acknowledge the European Synchrotron Radiation Facility for provision of synchrotron radiation facilities for experiment number SC5047.

Y. C., A. G., and F. R.-R. contributed equally to this work.

*Corresponding author.
chushkin@esrf.fr
†Corresponding author.
peter.schurtenberger@fkem1.lu.se

[1] J. Gunton, A. Shiryayev, and D. Pagan, *Protein Condensation: Kinetic Pathways to Crystallization and Disease* (Cambridge University Press, Cambridge, England, 2007).
[2] S. Bucciarelli, J. S. Myung, B. Farago, S. Das, G. A. Vliegenthart, O. Holderer, R. G. Winkler, P. Schurtenberger, G. Gompper, and A. Stradner, Sci. Adv. **2**, e1601432 (2016).
[3] G. Foffi, G. Savin, S. Bucciarelli, N. Dorsaz, G. M. Thurston, A. Stradner, and P. Schurtenberger, Proc. Natl. Acad. Sci. U.S.A. **111**, 16748 (2014).
[4] A. Stradner and P. Schurtenberger, Soft Matter **16**, 307 (2020).
[5] G. L. Hunter and E. R. Weeks, Rep. Prog. Phys. **75**, 066501 (2012).
[6] *Protein Self-Assembly*, edited by J. J. McManus (Springer, New York, 2019).
[7] M. Grimaldo, F. Roosen-Runge, F. Zhang, F. Schreiber, and T. Seydel, Q. Rev. Biophys. **52**, e7 (2019).
[8] A. Girelli, C. Beck, F. Bäuerle, O. Matsarskaia, R. Maier, F. Zhang, B. Wu, C. Lang, O. Czakkel, T. Seydel *et al.*, Mol. Pharma. **18**, 4162 (2021).
[9] G. Grübel, A. Madsen, and A. Robert, in *Soft Matter Characterization* (Springer, Netherlands, Dordrecht, 2008), pp. 953–995.
[10] P. Vodnala, N. Karunaratne, L. Lurio, G. M. Thurston, M. Vega, E. Gaillard, S. Narayanan, A. Sandy, Q. Zhang, E. M. Dufresne *et al.*, Phys. Rev. E **97**, 020601(R) (2018).
[11] J. Möller, M. Sprung, A. Madsen, and C. Gutt, IUCrJ **6**, 794 (2019).
[12] L. B. Lurio, G. M. Thurston, Q. Zhang, S. Narayanan, and E. M. Dufresne, J. Synchrotron Radiat. **28**, 490 (2021).
[13] A. Girelli, H. Rahmann, N. Begam, A. Ragulskaya, M. Reiser, S. Chandran, F. Westermeier, M. Sprung, F. Zhang, C. Gutt, and F. Schreiber, Phys. Rev. Lett. **126**, 138004 (2021).
[14] P. Raimondi, Synchrotron Radiat. News **29**, 8 (2016).
[15] S. Kuwamoto, S. Akiyama, and T. Fujisawa, J. Synchrotron Radiat. **11**, 462 (2004).
[16] T. Zinn, A. Homs, L. Sharpnack, G. Tinti, E. Fröjdh, P.-A. Douissard, M. Kocsis, J. Möller, Y. Chushkin, and T. Narayanan, J. Synchrotron Radiat. **25**, 1753 (2018).
[17] A. Tardieu, International Journal of Biological Macromolecules **22**, 211 (1998).
[18] T. Garting and A. Stradner, Small **14**, 1801548 (2018).
[19] See Supplemental Material at http://link.aps.org/supplemental/10.1103/PhysRevLett.129.238001 for protein purification; for description of radiation-induced relaxation process.
[20] A. Vrij, J. Chem. Phys. **71**, 3267 (1979).
[21] G. Williams and D. C. Watts, Trans. Faraday Soc. **66**, 80 (1970),
[22] M. Sutton, K. Laaziri, F. Livet, and F. Bley, Opt. Express **11**, 2268 (2003),
[23] E. Bartsch, M. Antonietti, W. Schupp, and H. Sillescu, J. Chem. Phys. **97**, 3950 (1992).
[24] F. Sciortino and P. Tartaglia, Adv. Phys. **54**, 471 (2005).

[25] L. Cipelletti, L. Ramos, S. Manley, E. Pitard, D. A. Weitz, E. E. Pashkovski, and M. Johansson, Faraday Discuss. **123**, 237 (2003).
[26] B. Ruta, F. Zontone, Y. Chushkin, G. Baldi, G. Pintori, G. Monaco, B. Rufflé, and W. Kob, Sci. Rep. **7**, 3962 (2017).
[27] G. Pintori, G. Baldi, B. Ruta, and G. Monaco, Phys. Rev. B **99**, 224206 (2019).
[28] Y. Chushkin, J. Synchrotron Radiat. **27**, 1247 (2020).
[29] B. Ruta, Y. Chushkin, G. Monaco, L. Cipelletti, E. Pineda, P. Bruna, V. M. Giordano, and M. Gonzalez-Silveira, Phys. Rev. Lett. **109**, 165701 (2012).
[30] P. Kwaśniewski, A. Fluerasu, and A. Madsen, Soft Matter **10**, 8698 (2014).
[31] K. Trachenko and A. Zaccone, J. Phys. Condens. Matter **33**, 315101 (2021).
[32] M. Weik, R. B. G. Ravelli, G. Kryger, S. McSweeney, M. L. Raves, M. Harel, P. Gros, I. Silman, J. Kroon, and J. L. Sussman, Proc. Natl. Acad. Sci. U.S.A. **97**, 623 (2000).
[33] C. M. Jeffries, M. A. Graewert, D. I. Svergun, and C. E. Blanchet, J. Synchrotron Radiat. **22**, 273 (2015).
[34] J. M. Gebicki and T. Nauser, Int. J. Mol. Sci. **23**, 396 (2021).
[35] C. L. Hawkins and M. J. Davies, Biochim. Biophys. Acta **1504**, 196 (2001).
[36] P. Vodnala, N. Karunaratne, S. Bera, L. Lurio, G. M. Thurston, N. Karonis, J. Winans, A. Sandy, S. Narayanan, L. Yasui *et al.*, AIP Conf. Proc. **1741**, 050026 (2016).
[37] M. Reiser, A. Girelli, A. Ragulskaya, S. Das, S. Berkowicz, M. Bin, M. Ladd-Parada, M. Filianina, H.-F. Poggemann, N. Begam *et al.*, Nat. Commun. **13**, 5528 (2022).
[38] M. Y. Lin, H. M. Lindsay, D. A. Weitz, R. C. Ball, R. Klein, and P. Meakin, Nature (London) **339**, 360 (1989).
[39] D. Stauffer and A. Aharony, *Introduction to Percolation Theory* (Taylor & Francis, London, 1994), revised 2n ed.
[40] Ozisik, Orlande, Colaco, and Cotta, *Finite Difference Methods in Heat Transfer, Second Edition* (CRC Press, Boca Raton, 2017).